

# Singularities of diffraction of Čerenkov radiation in a cholesteric liquid crystal

N. V. Shipov

All-Union Scientific Research Center for the Investigation of Surface and Vacuum Properties

(Submitted 12 September 1983)

Zh. Eksp. Teor. Fiz. 86, 2075–2090 (June 1984)

Čerenkov emission in cholesteric liquid crystals is examined theoretically for first-order reflection. The energy lost by a particle per unit frequency per unit azimuth angle as a result of this emission is shown to contain one forbidden band and two polarization-forbidden bands as well as, in general, six square-root singularities on the boundaries of these forbidden bands. It is shown that the radiation intensity on the boundaries of the reflection regions exhibits well-defined beats, and is proportional to the fourth power of the specimen thickness at the intensity maxima. When the particle moves at right-angles to the optical axis of the cholesteric, the differential radiative energy loss is a rapidly-varying function of the position of the particle trajectory.

## INTRODUCTION

It is well-known that the unusual optical properties of cholesteric liquid crystals (CLC) are due to their helicoidal structure which should, of course, also manifest itself in coherent emission by fast charged particles.<sup>1-3</sup> It has been shown<sup>1-3</sup> that, by analogy with the radiation emitted by charged particles in media with simply periodic dielectric properties (Refs. 4-7), Čerenkov radiation in cholesteric liquid crystals should take place not only in the direction of the well-known Čerenkov cone, but also in the direction of the so-called diffraction cone.

The existence of the square-root singularities and of a forbidden band in the radiative energy loss per unit frequency per unit azimuth angle was noted in Ref. 1, and simple expressions for the Čerenkov intensity along the helicoidal axis were reported in Ref. 2. More detailed information (both qualitative and quantitative) about the process was obtained by solving the problem of Čerenkov emission for second-order reflection in cholesteric liquid crystals. This has resulted in a relatively simple analytic expression for arbitrary directions of emission and particle velocity.<sup>3</sup> In particular, detailed analysis of the radiative loss<sup>3</sup> has shown that the appearance of bands into which Čerenkov radiation is forbidden in the case of infinite media is a common feature of periodic media. Simple analytic expressions were also obtained for the spectral density of radiation emitted into the Čerenkov and diffraction cones for a particle moving along a helicoidal CLC.

In this paper, we shall investigate the radiative loss and the angular, frequency, and polarization characteristics of Čerenkov radiation emitted in cholesteric liquid crystals under the conditions of first-order reflection. We shall determine the limits of the forbidden band for Čerenkov emission, and will analyze the corresponding boundary conditions in symmetric Bragg and Laue geometry. The differential radiative loss will be shown to be strongly dependent on the position of the particle trajectory when the particle moves at right-angles to the helicoidal (optical) axis of the cholesteric crystal.

## ČERENKOV RADIATION IN A CLC FOR PARTICLES MOVING AT AN ANGLE TO THE OPTICAL AXIS

*Directions of emission of Čerenkov radiation.* The analytic description of Čerenkov emission in a CLC becomes much more complicated for frequencies and angles satisfying the well-known Bragg condition

$$|k_0| = |k_0 + \tau| = \frac{\omega}{c} \varepsilon^{1/2} \left( 1 - \frac{\delta}{4} \cos^2 \theta \right), \quad (1)$$

where  $k_0$ ,  $k_1 = k_0 + \tau$  are the wave vectors at frequency  $\omega$  of the radiation emitted into the Čerenkov and diffraction cones (see Fig. 1),  $\bar{\varepsilon}$  is the average permittivity, and  $\delta$  is the dielectric anisotropy which is assumed to be small (typically  $\delta \sim 0.01-0.1$ ). In this paper, we shall concentrate on the study of Čerenkov radiation at frequencies and angles in the neighborhood of the values defined by the Bragg condition (1), where  $\tau = 4\pi/p$  is the reciprocal lattice vector and  $p$  is the pitch of the helix of the cholesteric. We recall that the Bragg frequencies and directions are geometrically determined by the intersection between the Čerenkov cone and

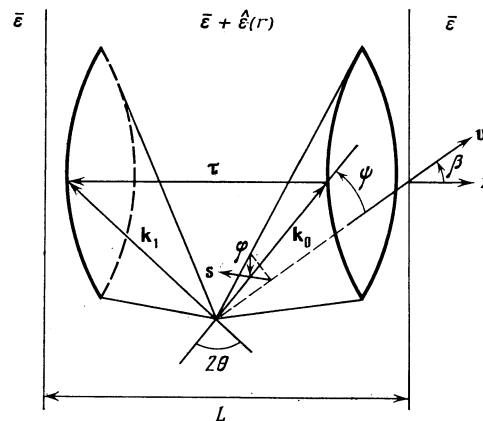


FIG. 1. Geometry of Čerenkov emission in a CLC when the charged particle moves at an angle to the helicoidal axis (z axis).

the plane that is perpendicular to the optical axis (to the vector  $\tau$ ) and cuts this axis at the point  $\tau/2$  (see Fig. 1).

The amplitude of the field due to a charged particle moving with velocity  $v > c/\varepsilon^{1/2}$  in an infinite crystal will be sought in the two-wave approximation

$$\mathbf{E}(r, t) = \frac{1}{(2\pi)^3} \int (\mathbf{E}_0 e^{i\mathbf{k}_0 \cdot \mathbf{r}} + \mathbf{E}_1 e^{i\mathbf{k}_1 \cdot \mathbf{r}}) d\mathbf{k}_0.$$

The components of the amplitudes  $\mathbf{E}_0, \mathbf{E}_1$  along the polarization unit vectors  $\pi_0, \pi_1, \sigma$  ( $\pi_0, \pi_1$  lie in the  $\mathbf{k}_0 \mathbf{k}_1$  plane, and  $\sigma$  is perpendicular to this plane) are solutions of the set of equations

$$\begin{aligned} (t+m)E_0^{\sigma-1/2}(1+m)E_1^{\sigma\rho+1/2}i(1+m)\sin\theta E_1^{\pi\rho} \\ = -4\pi i e \sigma \mathbf{v} (1+m) e^{-i\omega t} / \delta \omega \varepsilon, \\ (t-m)E_0^{\pi-1/2}i(1+m)\sin\theta E_1^{\sigma\rho-1/2}(1-m)E_1^{\pi\rho} \\ = -4\pi i e \pi_0 \mathbf{v} (1+m) e^{-i\omega t} / \delta \omega \varepsilon, \\ -1/2(1+m)E_0^{\sigma+1/2}i(1+m)\sin\theta E_0^{\pi+}(\eta+m)E_1^{\sigma\rho}=0, \\ -1/2i(1+m)\sin\theta E_0^{\sigma-1/2}(1-m)E_0^{\pi+}(\eta-m)E_1^{\pi\rho}=0, \end{aligned} \quad (2)$$

where  $\omega = \mathbf{k}_0 \mathbf{v}$ ,  $\rho = e^{-2i(\gamma - \Phi)}$ ,  $\Phi$  is the angle between the director and the  $x$  axis in the  $z = 0$  plane,  $\pi/2 - \theta, \gamma -$  are the polar and azimuthal angles of the wave vector  $\mathbf{k}_0$  in the coordinate frame whose polar axis lies along the optical axis,  $\psi, \varphi$  are the polar and azimuthal angles of the vector  $\mathbf{k}_0$  in the coordinate frame in which the polar axis lies along the velocity  $\mathbf{v}$ ,  $\eta = bt + 2\nu$ ,

$$\begin{aligned} m &= \cos^2 \theta (1 + \sin^2 \theta)^{-1}, \\ t &= -4(\psi - \psi_0) \operatorname{tg} \psi / \delta (1 + \sin^2 \theta), \\ \cos \psi_0 &= c/v \varepsilon^{1/2} (1 - 1/4 \delta \cos^2 \theta), \\ \sin \theta &= \cos \psi_0 \cos \beta - \sin \psi_0 \sin \beta \cos \varphi, \\ b &= -2 \sin^2 \beta \cos^2 \varphi + \sin 2\beta \operatorname{ctg} \psi_0 \cos \varphi + 1 \\ &\equiv \cos(\widehat{\mathbf{k}_1 \mathbf{s}}) / \cos(\widehat{\mathbf{k}_0 \mathbf{s}}), \end{aligned}$$

and the quantity  $\nu$  for fixed azimuth  $\varphi$  of the vector  $\mathbf{k}_0$  is given by

$$\begin{aligned} \nu &= 4 \sin^2 \theta (\omega - \omega_B) / \delta \omega_B (1 + \sin^2 \theta), \\ \omega_B &= c\tau / 2\varepsilon^{1/2} (1 - 1/4 \delta \cos^2 \theta) \sin \theta; \end{aligned} \quad (3a)$$

whereas, for fixed frequency,

$$\begin{aligned} \nu &= 4(\varphi - \varphi_B) \sin \theta \sin \beta \sin \varphi \sin \psi / \delta (1 + \sin^2 \theta), \\ \sin \theta_B(\varphi_B) &= c\tau / 2\omega \varepsilon^{1/2} (1 - 1/4 \delta \cos^2 \theta). \end{aligned} \quad (3b)$$

As was noted in Ref. 2, the Čerenkov radiation in a CLC in the neighborhood of the region defined by the Bragg condition (1) differs from the case of the usual homogeneous media<sup>8</sup> in that it is emitted into four cones separated by an angle interval  $\sim \delta$ . The directions of emission into the Čerenkov cone ( $\psi_i(\nu)$ ,  $i = 1 - 4$ ) are found by equating to zero the determinant of the set of equations (2), and are given by the roots  $t_i$  ( $n$ ) of the quartic

$$(t^2 - m^2)(\eta^2 - m^2) - (t - m^2)(\eta - m^2) = 0, \quad \eta = bt + 2\nu. \quad (4)$$

A diffraction cone corresponds to each of these four Čeren-

kov cones, in accordance with the condition  $\mathbf{k}_1 = \mathbf{k}_0 + \tau$ .

The radiation in each of these cones is, in general, elliptically polarized and the directions of the semiaxes of the polarization ellipse lie along the unit vectors  $\pi_{0,1}$  and  $\sigma$ . Using (2) and (4), we find that the ratios of semiaxes of the polarization ellipse in the directions of emission in the Čerenkov and diffraction cones are, respectively,

$$p_{0i} = \sin \theta \frac{t_i + m}{t_i - m}, \quad p_{1i} = \sin \theta \frac{bt_i + 2\nu + m}{bt_i + 2\nu - m}. \quad (5)$$

Depending on the particular geometry of the experiment (specific values of the angles  $\beta, \psi_0, \varphi_B$  that define the parameters  $b$  and  $m$ ), and depending on the frequency (azimuthal) detuning  $\nu$ , either two or four roots of (4) are complex. When there are four such roots, we have a band into which the emission is forbidden, i.e., a range of values of  $\nu$  that contains none of the angles  $\psi_i(\nu)$  ( $i = 1 - 4$ ) at which Čerenkov emission may take place.

The physical meaning of a band forbidden to Čerenkov radiation is most simply explained by considering a dispersion surface that defines the modulus of the wave vector of an eigenwave at a given frequency as a function of the direction of propagation and polarization (this surface is an ellipsoid in a birefringent medium and a sphere in an isotropic medium). The dispersion surface of a CLC in the neighborhood of the Bragg condition (1) has a rather complicated form and is described by (4) in which

$$\begin{aligned} t &= (1 - k_0^2 / \kappa^2) (1 + m) / \delta, \quad \eta = (1 - k_1^2 / \kappa^2) (1 + m) / \delta, \\ \kappa &= \frac{\omega}{c} \varepsilon^{1/2} \left( 1 - \frac{\delta}{4} \cos^2 \theta \right). \end{aligned}$$

The equation for the dispersion surface of the CLC is given in Ref. 9 in a somewhat different form.

Next, we note that the geometrical locus of the end point of the wave vector  $\mathbf{k}_0$  ( $\mathbf{k}_0 \cdot \mathbf{v} = \omega$ ), is a plane that is perpendicular to the axis of the Čerenkov cone and cuts this axis at  $k'_z = \omega/v$ . This plane cuts the dispersion surface of the cholesteric, in general, along four curves, and it is precisely to these curves that the four roots of (4) correspond (for a fixed ordinate in Fig. 3, these are four points on the curves). Hence, it is clear that the Čerenkov-forbidden band corresponds to the azimuth range  $\Delta\varphi = \varphi - \varphi_B \sim \delta$ , for which the direction of the vector  $\mathbf{s}$  (see Fig. 1) does not cut the dispersion surface of the CLC. For a fixed azimuth  $\varphi$ , the forbidden frequency band  $\Delta\omega/\omega \sim \delta$  can be interpreted in a similar way if we recall that a change in frequency corresponds to the stretching or contraction of the dispersion surface.

We shall show below how the limits of the Čerenkov-forbidden band can be calculated analytically in the most general case of arbitrary direction of emission (arbitrary angles  $\beta$  and  $\varphi$ ) and arbitrary particle energies (arbitrary angle  $\psi_0$  of the Čerenkov cone). We note that (4) is quadratic in  $\nu$ , and its solutions are

$$\begin{aligned} 2\nu_{\pm} &= -bt + \eta_{\pm}, \\ \eta_{\pm} &= \{t - m^2 \pm [(t - m^2)^2 + 4m^2(t^2 - t)(t^2 - m^2)]^{1/2}\} / 2(t^2 - m^2). \end{aligned} \quad (6)$$

The quantities  $\nu_{\pm}(t)$  found in this way define the frequency

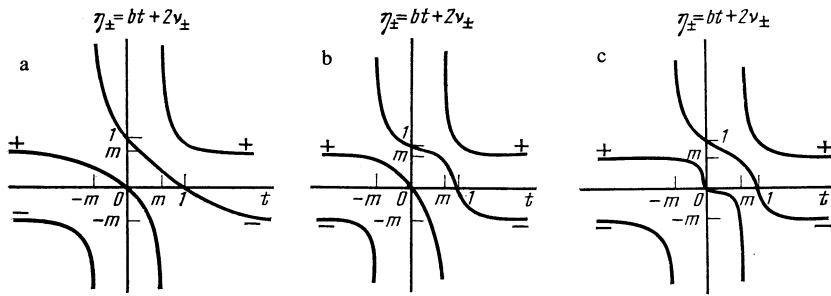


FIG. 2. The roots  $\eta_{\pm}$  as functions of the polar angle ( $\psi - \psi_0 \approx t$ ): a— $32^\circ \leq \theta < 90^\circ$ , b— $25^\circ \leq \theta \leq 32^\circ$ , c— $0 < \theta \leq 25^\circ$ .

(azimuth) of the Čerenkov emission maxima. The solutions of the inhomogeneous set (2) are then infinite. We recall that fixed  $t$  in (6) corresponds to a fixed polar angle  $\varphi$  of the wave vector  $\mathbf{k}_0$ . The ratios of the semiaxes of the polarization ellipse at the maxima of  $v = v_{\pm}(t)$  are then given by expressions analogous to (5), namely,

$$p_{0\pm} = \sin \theta \frac{t+m}{t-m}, \quad p_{1\pm} = \sin \theta \frac{\eta_{\pm}+m}{\eta_{\pm}-m}. \quad (7)$$

Figure 2 shows a graph of the roots  $\eta_{\pm}(t)$ . By adding the graphs of  $\eta_{\pm}(t)$  to the straight line  $\eta = -bt$ , we obtain the function  $2v_{\pm}(t)$ . Analysis of the  $\eta_{\pm}(t)$  curves (see Fig. 2) shows that the forbidden band appears only for  $b < 0$ , when  $v_{\pm}(t)$  have characteristic maxima or minima. In Fig. 2,

$$t = -2(1+m)(\psi - \psi_0) \operatorname{tg} \psi_0 / \delta, \quad \cos \psi_0 = c/v\epsilon^{1/2}(1 - 1/4\delta \cos^2 \theta).$$

The intervals of values of  $v$  in which the line  $v = \text{const}$  does not cut the  $v_{\pm}(t)$  and  $v - (t)$  curves define the Čerenkov-forbidden band:

$$\max(v_+^{\max}, v_-^{\max}) < v < \min(v_+^{\min}, v_-^{\min}). \quad (8)$$

The above procedure of finding the forbidden band is illustrated for the special case  $b = -1$  in Fig. 3. The figure also shows the limits of the forbidden band for Čerenkov emission. In this figure,

$$v_{\pm}^p = 1/2[-1 \pm (1+8m^2)^{1/2}], \\ v_{\pm}^r = 1/4 \pm 1/4 m^{-1}[(1-m^2)(4m^2-1)]^{1/2}.$$

*Spectral and angular distribution of Čerenkov radiation in a CLC.* As noted above, the intervals of values of  $v$  in which all four roots  $t_i(v)$  ( $i = 1-4$ ) of (4) are complex, define the Čerenkov-forbidden band in which the wave intensity does not increase with increasing specimen thickness. We may therefore assume that  $d^2W/d\omega d\Omega = 0$ , in such inter-

vals, where  $W$  is the energy radiated by the charged particles per unit path and  $d\Omega = \sin\psi d\psi d\varphi$  is the solid-angle element. Integration of  $d^2W/d\omega d\Omega$  with respect to the polar angle  $\psi$  yields the radiation loss per unit frequency per unit azimuth,  $d^2W/d\omega d\varphi$ , and this also vanishes in the forbidden band. Integration of  $d^2W/d\omega d\varphi$  with respect to  $\varphi$  yields the spectral density of the radiative loss which, as will be seen below, differs from the spectral density of radiative loss in a homogeneous medium with refractive index  $\epsilon^{1/2}$  by a very small quantity (in general,  $\sim \delta$ ). Thus, from the practical point of view, it is interesting to examine the differential loss  $d^2W/d\omega d\varphi$ , which, in contrast to  $dW/d\omega$ , is very different from the corresponding radiative loss in the homogeneous medium:

$$\frac{d^2W_0}{d\omega d\varphi} = \frac{e^2\omega}{2\pi c^2}(1 - c^2/v^2\epsilon). \quad (9)$$

In particular, integrating (9) with respect to  $\varphi$  between 0 and  $2\pi$ , we obtain the well-known Tamm-Frank formula.<sup>8</sup>

We note that  $d^2W/d\omega d\psi$  can be calculated analytically with the aid of the expressions for  $v_{\pm}(t)$  (6) in the most general case by integrating  $d^2W/d\omega d\Omega$  with respect to  $\varphi$  between 0 and  $2\pi$ . The resulting divergences at the points  $t = \pm m$  correspond to the generation of linearly  $\pi$ - or  $\sigma$ -polarized waves [see also (7)] on the Čerenkov cone outside the Bragg condition (1). Thus, the intensity emitted at a fixed polar angle  $\psi$  describes the Čerenkov effect rather than its diffraction properties. More accurate expressions can be obtained by integrating over the Čerenkov cone without assuming that the deviation of the azimuth angle  $\varphi$  from the Bragg angle  $\varphi_B$  is small [see also (3b)].

At this point, it is appropriate to note that, when the deviation of the polar angle  $\psi$  from the angular aperture  $\psi_0$  of the Čerenkov cone is not small (large values of  $t$ ), the radiation is emitted mainly into the diffraction cone and is linearly polarized along the unit vectors  $\pi_1$  and  $\sigma$  for

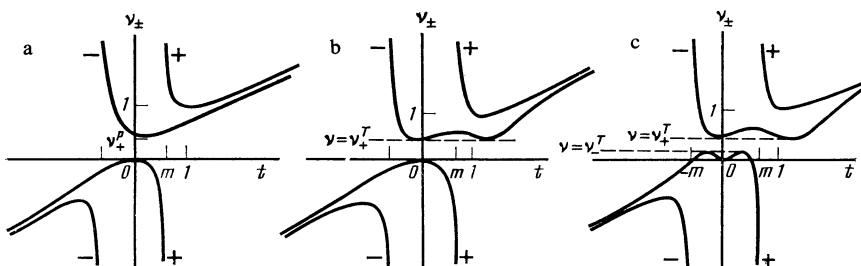


FIG. 3. Determination of the boundaries of the Čerenkov-forbidden band. The frequency (azimuthal) detuning  $v_{\pm}(t)$  corresponding to emission maximum is shown as a function of the polar angle for  $b = 1$ . The curves are sections of the CLC dispersion surface by the  $\omega = k_0v$  plane (the  $t$  axis lies along the unit vector  $\mathbf{s}$ , and the ordinate axis along the unit vector  $\mathbf{v}(\mathbf{v} \perp \mathbf{s})$ ): a— $32^\circ \leq \theta < 90^\circ$ , b— $25^\circ \leq \theta \leq 32^\circ$ , c— $0 \leq \theta \leq 25^\circ$ .

$\eta_{\pm} = \pm m$ , respectively [see (7)]. This is the well-known structural Čerenkov radiation (see, for example, Ref. 4) and its intensity ( $\sim \delta^2$ ) is much lower than that of the Čerenkov radiation.

We now turn to the direct evaluation of the radiative loss  $d^2W/d\omega d\varphi$ . We shall suppose that the medium produces infinitesimal attenuation which we shall take into account later in the principal values of the permittivity tensor  $\epsilon_k$  ( $k = 1 - 3$ ) by introducing infinitesimal imaginary parts  $\epsilon_k^* = \gamma' \epsilon_k$ , where  $\gamma' \ll 1$ . This is equivalent to the addition of a small component  $\bar{\epsilon}''$  (positive for  $\omega > 0$ ) to  $\bar{\epsilon}$ . The differential radiative loss  $d^2W/d\omega d\varphi$  is then found by integrating with respect to the polar angle  $\psi$  by analogy with Refs. 3 and 8 and, in general, can be expressed in terms of the roots  $t_i$  ( $\nu$ ) ( $i = 1 - 4$ ) of (4) [see also (5)].

We shall not write out the relatively unwieldy general expressions, and will merely analyze the radiative loss of a particle for directions  $\mathbf{k}_0$  on the Čerenkov cone that satisfy the condition  $b(\varphi) = -1$ . For an arbitrary direction of the particle velocity vector, there are two symmetric angles  $\varphi$  for which  $b = -1$ , so that (4) reduces to a biquadratic equation and its roots are

$$t_i(\nu) = \nu \pm (\nu^2 + m^2 - 1/2 \pm r)^{1/2}, \quad (10)$$

$$r = 1/2 [m^2(4\nu - 1)^2 + (m^2 - 1)(4m^2 - 1)]^{1/2}.$$

We note that the polarization characteristics (5) of the wave emitted in the  $i$ th direction ( $i = 1-4$ ) will, of course, coincide with the polarization characteristics of one of the eigenwaves of the CLC defined by the same point on the dispersion curve that is reached by the end point of the wave vector  $\mathbf{k}_0$ . However, the characteristic feature of this case ( $b = -1$ ) is that the polarization characteristics (5) of radiation in the  $i$ th direction are exactly the same as the polarization characteristics of the fully defined  $i$ th eigenwave of the CLC ( $i = 1 - 4$ ) throughout the range of  $\nu$  when the boundary-value problem is solved for the symmetric Bragg geometry.<sup>9</sup> The tangential components of the wave vectors on the boundaries of the planar CLC specimen are then assumed to coincide. It is appropriate at this point to recall that, of the four CLC eigenwaves<sup>9</sup> in symmetric Bragg geometry, only two [they correspond to different signs in front of the inner radical  $r$  in (10)] are different (for equal tangential components of the wave vectors, they correspond to different branches of the dispersion curve,  $\nu < 0$ ,  $\nu > \nu_+$ ). The other two eigenwaves differ from those just mentioned only by the direction of propagation, which corresponds to a change in the sign in front of the outer radical in (10). On the other hand, a change in the direction of propagation of the eigenwave is described by the replacements  $\mathbf{k}_0^+ \rightarrow \mathbf{k}_1^-$ ,  $\mathbf{k}_1^+ \rightarrow \mathbf{k}_0^-$ . The same branch of the dispersion curve corresponds to CLC eigenwaves differing only by the direction of propagation. Thus, the case  $b = -1$  that we have been considering enables us to conclude that the cholesteric crystal has polarization-forbidden bands for Čerenkov emission, which correspond to intervals of  $\nu$  with two complex roots (10) of (4).

The expression for the radiation loss will now be written in the form of a sum of two terms (instead of the four corresponding to each direction of emission,  $i = 1-4$ ). Each of

these terms corresponds to physically different CLC eigenwaves and different signs in front of the inner radical  $r$  in (10):

$$\frac{d^2W}{d\omega d\varphi} = \frac{d^2W_0}{d\omega d\varphi} w, \quad w = (f_+^\sigma + f_-^\sigma) \xi_\sigma + (f_+^\pi + f_-^\pi) \xi_\pi,$$

$$f_{\pm}^\sigma = \frac{4m\nu^2 + (4m^2 - m)\nu - m^2(1 - m) - m \pm 2(\nu + m)r}{(\pm 4r) \left( \nu^2 + m^2 - \frac{1}{2} \pm r \right)^{1/2}}, \quad (\nu > 1),$$

$$\xi_\sigma = (\sigma\nu)^2 / (\nu^2 - c^2/\bar{\epsilon}), \quad \xi_\pi + \xi_\sigma = 1, \quad (11)$$

where  $f_{\pm}^\pi$  is expressed in terms of  $f_{\pm}^\sigma$  by replacing  $m$  with  $-m$ . When the expression under the square root in at least one of the radicals in (10) and (11) becomes negative as  $\nu$  is reduced (this corresponds to the forbidden band for the emission of the particular CLC eigenwave), the associated function  $f_+$  or  $f_-$  is set equal to zero in (11).

When Čerenkov radiation is emitted along the helicoidal axis ( $m = 0$ ,  $\beta = \psi_0$ ,  $\xi_\sigma = 0$ ), we have  $f_+^\pi = 1/2$ ,  $f_-^\pi = \nu/2(\nu^2 - 1)^{1/2}$ , so that the signs in front of the radical in (10) and (11) describe the undiffracted (diffracted) circularly polarized wave. Integration with respect to  $\nu$  then readily shows that the integrated radiative losses corresponding to the emission of the diffracted (right circularly polarized) and undiffracted (left circularly polarized) waves are equal. The corresponding intensities emitted into the Čerenkov and diffraction cones are calculated in Ref. 2 for a plane CLC layer.

In the limit of large deviations from the Bragg condition (1) ( $|\nu| \gg 1$ ) for waves propagating at an angle to the optical axis, the positive and negative signs correspond to the ordinary and extraordinary linearly polarized waves. For the ordinary wave, polarized in the direction of the unit vector  $\sigma$ , we have  $f_+^\sigma = 1$ ,  $f_+^\pi = 0$  ( $\nu \gg 1$ , see Fig. 4a) whereas, for the extraordinary wave polarized along the unit vector  $\pi_0$ , we have  $f_-^\sigma = 0$ ,  $f_-^\pi = 1$ . Thus,  $f_{\pm}^{\sigma,\pi}$  describe the contribution of the unit vectors  $\pi$  and  $\sigma$  to the radiative loss for physically different eigenwaves of the cholesteric (see Fig. 4a).

Depending on the parameter  $m$ , i.e., the angle  $2\theta$  between  $\mathbf{k}_0$  and  $\mathbf{k}_1$ , which for the emission directions that we are considering is determined by the angles  $\beta$  and  $\psi_0$ , the two polarization-forbidden bands turn out to be contiguous with the Čerenkov-forbidden band (Fig. 4b) or are separated from it (Figs. 4c and d). This is responsible (Fig. 4e) for the six square-root singularities in the differential emission  $d^2W/d\omega d\varphi$ . However, the particle loss integrated with respect to frequency (azimuthal angle) is no different from the corresponding integrated loss in the homogeneous medium with refractive index  $\bar{\epsilon}^{1/2}$ , which is readily verified by integrating  $W$  with respect to  $\nu$  for example, for  $\sin\theta = 1/\sqrt{3}$ <sup>11</sup> (this was demonstrated by V. P. Orlov for emission in the direction of the helicoidal axis<sup>2</sup>). Similar conclusions have been reported<sup>1,3,5,7</sup> for the simplest axially symmetric Čerenkov geometry for particles moving along the reciprocal lattice vector of a periodic structure.

*Boundary-value problem.* Consider the radiation from a charged particle in a planar cholesteric layer in a homogeneous medium with refractive index  $\bar{\epsilon}^{1/2}$  (the helicoidal axis of the planar CLC specimen is perpendicular to the surfaces of

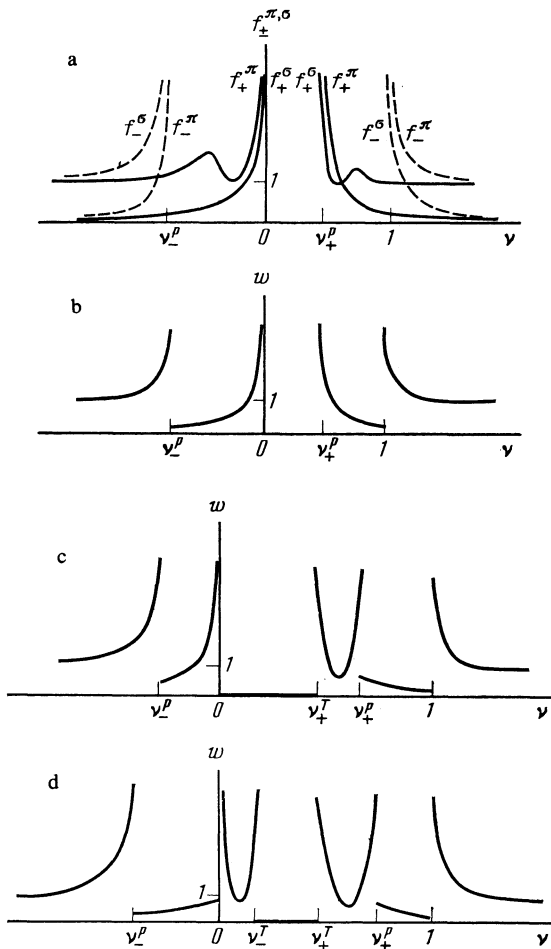


FIG. 4. Frequency (azimuthal) dependence of the differential radiation loss  $d^2W/d\omega d\varphi$  for  $b = -1$ : a—frequency dependence of  $f_{\pm}^{\pi, \sigma}$  for  $\theta = \arcsin 3^{-1/2} > 32^\circ$ . The function  $w(\nu)$  is shown for: b— $32^\circ < \theta \leq 90^\circ$ , c— $25^\circ \leq \theta \leq 32^\circ$ , d— $0 < \theta \leq 25^\circ$ .

the layer). The field in the crystal will be sought in the form of the sum of solutions of the inhomogeneous set of equations (2) and a superposition of four CLC eigenwaves [solution of the homogeneous set of equations (2)]. Since we wish to exhibit the essential diffraction effects, we shall suppose that the conditions for Čerenkov emission will be satisfied in the cholesteric layer of thickness  $L$ , but not satisfied in the outer medium<sup>2</sup> (for example, the charge of the particle will be "turned on" only during its passage through the cholesteric). In this formulation, the boundary conditions are completely analogous to the boundary conditions in x-ray optics.<sup>2,3,9,10</sup> In particular, the boundary conditions for x-ray emission by ultrarelativistic particles in perfect crystals are given in Ref. 11. Here, however, we note that the well-known Tamm-Frank formula<sup>8</sup> can also be deduced by solving the boundary-value problem formulated above.<sup>2,3</sup>

Thus, the particular feature of the boundary-value problem solved below is that we are able to exclude transition radiation (see, for example, Refs. 4 and 12) and the effect of dielectric reflection.<sup>9</sup>

Equating the tangential components of the electric field on either side of the surface of the crystal, we obtain the

following expressions for the amplitudes of the field radiated into the Čerenkov cone ( $E_c$ ) and the diffraction cone ( $E_d$ ):

$$E_d^\sigma = D^{-1} \begin{pmatrix} a_{11} & a_{12} & a_{13} & a_{14} & E_0^\sigma \\ a_{21} & a_{22} & a_{23} & a_{24} & E_0^\pi \\ a_{31}\gamma_1 & a_{32}\gamma_2 & a_{33}\gamma_3 & a_{34}\gamma_4 & E_1^\sigma\gamma_0 \\ a_{41}\gamma_1 & a_{42}\gamma_2 & a_{43}\gamma_3 & a_{44}\gamma_4 & E_1^\pi\gamma_0 \\ a_{31} & a_{32} & a_{33} & a_{34} & E_1^\sigma \end{pmatrix}, \quad (12)$$

where

$$\gamma_j = e^{-ia(m+j)}, \quad \gamma_0 = e^{-ia(m+t)},$$

$$q_j = \Delta \pm [\Delta^2 + m^2 - 1/2 \pm r(\Delta)]^{1/2} \quad (j=1-4),$$

$$t+m = -2(1+m) \sin \theta_e \sin \psi^e (\psi^e - \psi_0^e) / \delta \cos \beta,$$

$$\cos \psi_0^e = c/v\epsilon^{1/2},$$

$$a = \delta \kappa_e L / 2(1+m) \sin \theta_e, \quad \kappa_e = \omega \epsilon^{1/2} / c,$$

$$\sin \theta_e = \cos \psi_0^e \cos \beta - \sin \psi_0^e \sin \beta \cos \varphi_e,$$

$a_{ij}$  are the amplitudes of the eigenwaves in the cholesteric<sup>9</sup> ( $i, j = 1-4$ ):

$$a_{1j} = (q_j - m)(\eta_j^2 - m^2), \quad a_{3j} = (\eta_j - m)(q_j - m^2),$$

$$a_{2j} = i \sin \theta (q_j + m)(\eta_j^2 - m^2),$$

$$a_{4j} = i \sin \theta (\eta_j + m)(q_j - m^2), \quad \eta_j = 2\Delta - q_j,$$

$E_0, E_1$  are the solutions of the inhomogeneous set (2),  $D$  is expressed in terms of the determinant (12) by crossing out the fifth row and the fifth column, and  $E_d^\sigma, E_c^\sigma, E_c^\pi$  are expressed in terms of  $E_d^\sigma$  by replacing the bottom row of the determinant (12), respectively, with  $a_{4j}, E_1^\pi a_{ij}\gamma_j, E_0^\sigma\gamma_0; a_{2j}\gamma_j, E_0^\pi\gamma_0$ . The parameter  $\Delta$  representing the departure from the Bragg conditions and defining the cholesteric eigenwaves can be expressed in terms of the polar ( $\psi^e$ ) and azimuthal ( $\varphi_e$ ) angles of the wave vector  $\kappa_e$  of the wave leaving the crystal:

$$\Delta = A(t+m) + v,$$

$$A = (\sin \psi_0^e \cos \beta + \cos \psi_0^e \cos \varphi^e \sin \beta) \cos \beta / \sin \psi_0^e,$$

where, for fixed  $\varphi^e$

$$\nu = 4 \sin^2 \theta_e (\omega - \omega_B) / \delta \omega_B (1 + \sin^2 \theta_e), \quad (13a)$$

$$\omega_B = c\tau / 2\epsilon^{1/2} (1 - 1/4 \delta \text{ctg}^2 \theta_e) \sin \theta_e;$$

and for fixed frequency  $\omega$

$$\nu = 4 \sin \theta_e \sin \beta \sin \psi_0^e \sin \varphi_B^e (\varphi^e - \varphi_B^e) / \delta (1 + \sin^2 \theta_e), \quad (13b)$$

$$\sin \theta_B^e (\varphi_B^e) = c\tau / 2\omega \epsilon^{1/2} (1 - 1/4 \delta \text{ctg}^2 \theta_e).$$

The directions of emission (angles  $\psi_i^e(\nu), i = 1-4$ ) of the Čerenkov radiation from the CLC specimen of finite dimensions are, as before, given by (4) in which we must substitute  $\eta = 2\Delta - t = b_e t + 2(\nu + Am)$ , where  $b_e = 2A - 1$ .

The amplitudes of the field radiated into the Čerenkov cone oscillate as we depart from the Bragg condition ( $|\nu| \gg 1$ ), tending (to within  $\sim \delta$ ) to the expressions for the amplitudes of the Čerenkov radiation in birefringent media,<sup>8</sup> whereas

the field radiated into the diffraction cone oscillates and decays as  $\nu^{-1}$ .

Diffraction effects become important for  $|\nu| \sim 1$ . Let us examine the conditions under which the emission of Čerenkov radiation occurs at the boundaries of diffractive reflection,  $\Delta = \Delta^{p,T}$ . Using the known<sup>9</sup> boundary values  $\Delta^{p,T}$  together with (4), we find that the corresponding frequency (azimuth) detuning is

$$\nu = \nu^{p,T} = \Delta^{p,T} - A(t^{p,T} + m), \quad (14)$$

and the polar angles of the direction of emission of the radiation, determined by the parameter  $t$ , are given by

$$t = t^p = \Delta^p \quad \text{for} \quad \Delta^p = 0, 1, \quad \frac{1}{2} [-1 \pm (1 + 8m^2)]^{1/2}, \quad (15a)$$

$$t = t^T = \Delta^T \pm [(\Delta^T)^2 + m^2 - 1/2]^{1/2}$$

$$\text{for} \quad \Delta^T = \frac{1}{4} \pm \frac{1}{4m} [(1 - m^2)(4m^2 - 1)]^{1/2}. \quad (15b)$$

We must now examine in greater detail the nature of the beats near some particular ( $\Delta = \Delta^p$  or  $\Delta = \Delta^T$ ) reflection boundary. The intensity of the emitted waves for small differences  $\Delta - \Delta^{p,T}$  which, in turn, are determined by small differences  $\nu - \nu^{p,T}$  or  $t - t^{p,T}$  satisfying the condition

$$L(k_{01z} - k_{02z}) = a(q_1 - q_2) = 2\pi n \quad (n = \pm 1 \pm 2 \dots), \quad (16)$$

reaches the maxima  $\sim L^4 \delta^2 / p^2$ . The frequency (angular) interval between the maxima is  $\Delta\omega/\omega \sim \delta^{-1}(p/L)^2$ , and the frequency (angular) width of these maxima is  $\sim \delta^{-2}(p/L)^3$  (see also Ref. 10). The indices  $j = 1, 2$  describe the two eigenwave solutions for the CLC which coincide on the boundary  $\Delta^p$  or  $\Delta^T$ .

The polarization characteristics at the maxima (16) will, in general, depend on the thickness, but the result becomes much simpler when the boundary  $\Delta^p$  lies in the region of select (polarization selective) reflection for which the wave vectors  $\mathbf{k}_{0j}$  ( $j = 3, 4$ ) of the two other eigenwaves of the cholesteric

$$e_j = (a_{1j}\sigma + a_{2j}\pi_0) e^{i k_{0j} r} + (a_{3j}\sigma + a_{4j}\pi_1) e^{i(k_{0j} + \tau)r}$$

are complex. Suppose, for example, that  $j = 3$  and  $j = 4$  correspond to CLC eigenwaves that respectively grow and decay exponentially with depth in the crystal (along the  $z$  axis in Fig. 1). The polarization of the radiation leaving the planar CLC layer is then orthogonal to the wave that grows exponentially in the direction of propagation in the  $j$ th eigenwave solution ( $j = 3, 4$ ):

$$E_d^{\pi} / E_d^{\sigma} = - (a_{3i} / a_{4i})^* = E_c^{\pi} / E_c^{\sigma} = - (a_{13} / a_{23})^*$$

$$= \frac{i}{\sin \theta_e} \frac{m + i(1 - 2m^2)^{1/2}}{m - i(1 - 2m^2)^{1/2}}, \quad \Delta \rightarrow \Delta^p = 0 \quad (0 < m^2 < 1/2);$$

$$E_d^{\pi} / E_d^{\sigma} = - (a_{3i} / a_{4i})^* = E_c^{\pi} / E_c^{\sigma} = - (a_{13} / a_{23})^*$$

$$= \frac{1}{i \sin \theta_e} \frac{\Delta^p - m - i((1 + 8m^2)^{1/2} - 6m^2)^{1/2}}{\Delta^p + m - i((1 + 8m^2)^{1/2} - 6m^2)^{1/2}}, \quad (17)$$

$$\Delta \rightarrow \Delta^p = \frac{1}{2} (-1 + (1 + 8m^2)^{1/2}), \quad 0 < m^2 < (2 + \sqrt{13})/18.$$

The frequency widths of the above maxima are relatively small. For example, for the characteristic dimensions of

cholesteric crystals ( $\delta \sim 0.1$  and  $L \sim 100$  m), we have  $\Delta\omega/\omega \sim 10^{-4}$  and the intensity at maximum exceeds the characteristic intensity outside the region of selective absorption (where  $I_0 \sim L^2$ ) by a factor of the order of 100. We note that absorption begins to affect the above beats near the diffractive-reflection boundary even for thickness  $L \sim p(\delta\epsilon'')^{-1/2}$ , i.e., much smaller than the absorption length (see also Ref. 13).

The above intensity beats on the diffractive reflection boundaries are seen only in Bragg geometry and are absent in Laue geometry. Their existence is unrelated to the restriction on the values of the parameter  $b$ . In particular, the intensity beats occur for  $b > 0$ , when the frequency spectrum of the differential loss  $d^2W/d\omega d\varphi$  does not contain Čerenkov-forbidden bands or square-root divergences on the boundaries of the forbidden bands. It is, however, important to note that the intensity beats on the diffractive-reflection boundary do not produce an increase in the intensity of Čerenkov radiation-integrated over the frequency (angles  $\varphi^e$  and  $\psi^e$ ) in the general case of a spatially periodic medium. The most promising way of detecting and then investigating in detail the above maxima is to consider the motion of a particle along the helicoidal axis of the cholesteric, since the angular distribution of the emitted intensity is then axially symmetric (independent of the azimuth  $\varphi$ ); in this case,  $b = b_e = A = 1$ .

As regards the Čerenkov-forbidden bands, which appear for  $b > 0$ , these naturally manifest themselves in the intensity integrated over the polar angle  $\psi^e$  and emerging from the CLC specimen of finite thickness, whilst the radiation intensity on the boundaries of the forbidden bands is much higher than the intensity in the homogeneous medium. In the Laue geometry, for example, the difference is  $\sim (\delta L/p)^{1/2}$  (see below).

Let us consider, for example, this type of increase in the integrated intensity for the special case where  $b_e = -1$  ( $A = 0$ ). The geometrical meaning of the condition  $b_e = -1$  is as follows: the end-point of the wave vector  $\kappa_e$  describes the arc of a circle as the polar angle  $\psi^e$  is varied, and this arc touches the plane perpendicular to the helicoidal axis (the vector  $\tau$ ) when  $b_e = -1$ . Since the parameter  $\Delta$ , in terms of which the intrinsic polarizations of the CLC are expressed, is determined by the component of  $\kappa_e$  along the vector  $\tau$  (Ref. 9), we have  $\Delta \equiv \nu$  in this case, and  $\Delta$  turns out to be independent of  $\psi^e$ , so that the direction of emission and the CLC eigenwaves are determined by the same equation (4) in which  $\eta = 2\nu - t$ . The region of nonselective (selective) absorption then coincides with the forbidden (polarization-forbidden) band for the emission of Čerenkov radiation (Figs. 4b, c, and d). The emitted intensities integrated over the polar angle  $\psi^e$  exhibit intensive beats on the boundaries of the forbidden bands and reach values of the order of  $\sim L^3(\delta/p)^2$  at the maxima. A simple case of emission along the helicoidal axis was examined in Ref. 2. In particular, the expressions for the emitted intensity obtained in Ref. 2 do, in fact, describe the increase in Čerenkov radiation, integrated over the polar angle  $\psi_e$ , on the boundary of the polarization-forbidden band.

Next, we note that the intensities averaged over the frequency interval between the maxima increase in accordance

with the formulas

$$I_c, I_d \sim I(\nu - \nu^{p,T})^{-1/2}, \quad I = Le^2 \omega (1 - c^2/\nu^2 \epsilon) / 2\pi c^2$$

up to values  $\nu - \nu^{p,T} \sim (\delta L/p)^{-2}$  corresponding to the absolute maximum.

We note in conclusion that orthogonality conditions analogous to (17) can be shown to be satisfied for the wave transmitted by the CLC not only on the boundary but throughout the region of selective absorption in the corresponding reflection and transmission optical problem (independently of the polarization of the wave incident on the crystal).

### ČERENKOV EMISSION BY A PARTICLE MOVING AT RIGHT-ANGLES TO THE HELICOIDAL AXIS OF THE CHOLESTERIC CRYSTAL

**Radiation loss.** The Čerenkov radiation emitted by a particle moving at right-angles to the optical axis in a CLC has a number of specific properties. For example, the directions of emission into the Čerenkov and diffraction cones are found to coincide (the diffraction cone is, as it were, inscribed into the Čerenkov cone). This means that, when the radiation loss and polarization characteristics of the radiation emitted in the direction with azimuth  $\varphi$  are calculated, it is important to take into account the corresponding characteristics in the direction with azimuth  $\pi - \varphi$  (see Fig. 5).

Using the solution of (2) and combining the field amplitudes of radiation emitted in directions with azimuths  $\varphi$  and  $\pi - \varphi$ , in which the wave vectors coincide, i.e.,  $\mathbf{k}_0(\varphi) = \mathbf{k}_1(\pi - \varphi)$ ,  $\mathbf{k}_0(\pi - \varphi) = \mathbf{k}_1(\varphi)$ , we can readily verify that the polarization characteristics in the direction of emission are, as before, given by (5), and  $b = -\cos 2\varphi$ .

We now reproduce the expression for the radiation loss at the point on the cone with azimuth  $\varphi = 0$  (the plane of diffraction scattering is then coincident with the plane defined by the helicoidal axis and the velocity vector; see Fig. 5):

$$\frac{d^2 W}{d\omega d\varphi} = \frac{d^2 W_0}{d\omega d\varphi} w, \quad w = 2(f_+^\pi + g_+ \cos 2\Phi + f_-^\pi + g_- \cos 2\Phi),$$

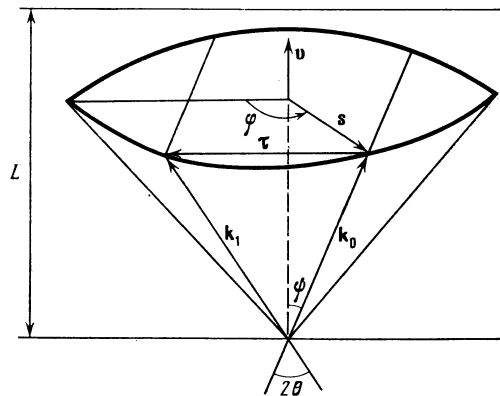


FIG. 5. Geometry of Čerenkov emission in a CLC when the charged particle moves at right-angles to the helicoidal axis.

$$g_\pm = \frac{(1-m)(1+4m\nu \mp 2r)}{(\pm 8r) \left( \nu^2 + m^2 - \frac{1}{2} + r \right)^{1/2}} (\nu > 1), \quad m = \frac{\cos^2 \psi_0}{1 + \sin^2 \psi_0}, \quad (18)$$

where  $f_\pm^\pi$  is given by (11) and, as  $\nu$  is reduced, the quantities  $f_\pm^\pi, g_\pm$  are assumed by analogy with (11) to be equal to zero in the Čerenkov-forbidden bands and change sign on the other side of the corresponding boundary of the forbidden band (see Fig. 6a, where the solid line shows the function  $\omega_\pm = 2(f_\pm^\pi + g_\pm \cos 2\Phi)$  as the particle travels along the long axes of the molecules,  $\Phi = 0$ ). The frequency dependence of the differential radiation loss (18) is sensitive to the position of the charged-particle trajectory in space, i.e., to the angle  $\Phi$  (see Figs. 6b, c, and d) at which the particle crosses the long axes of the molecules (the director) as it moves in the plane perpendicular to the helicoidal axis of the cholesteric. In particular, when the particle moves along the director ( $\Phi = 0$ , see solid curve in Figs. 6b, c, and d, the

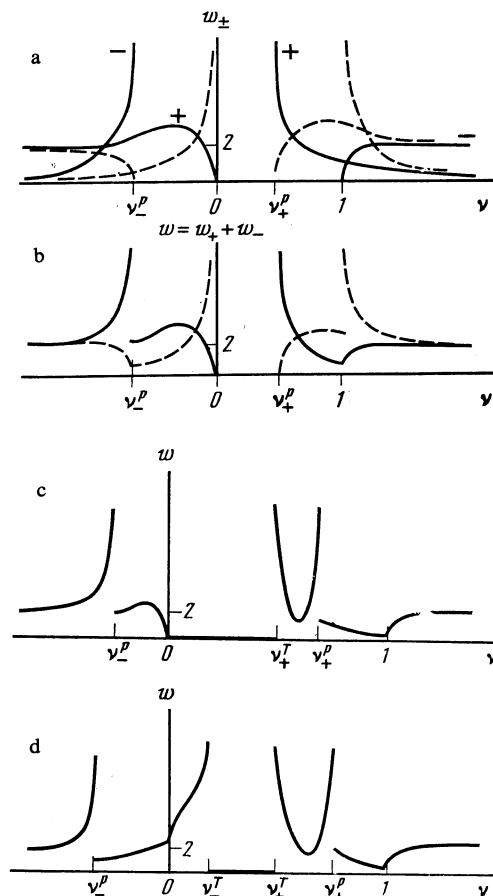


FIG. 6. Frequency dependence of the differential loss  $d^2 W/d\varphi d\omega$  when the charged particle moves at right-angles to the helicoidal axis of the CLC. Solid curve—particle moving along the long axes of the molecule,  $\Phi = 0$ ; broken line—motion at right-angles to the long axes of the molecule,  $\Phi = \pi/2$ ,  $\varphi = 0$ , see Fig. 5; a— $w_\pm = 2(f_\pm^\pi + g_\pm \cos 2\Phi)$  (solid curves,  $25^\circ \leq \psi_0 \leq 32^\circ$ ) as a function of  $\nu$ , and  $w_\pm = 2(f_\pm^\pi + g_\pm \cos 2\Phi)$  (broken curves,  $\Phi = \pi/2$ ). The figure also shows the general shape of the frequency dependence  $w(\nu)$  for the following values of the angle  $\psi_0$ : b— $32^\circ \leq \psi_0 < 90^\circ$ , c— $25^\circ \leq \psi_0 \leq 32^\circ$ , d— $0 < \psi_0 \leq 25^\circ$ .

differential radiation loss (18) vanishes on the  $\nu = 0$  boundary of the Čerenkov-forbidden band and becomes infinite on the boundaries  $\nu = \nu_{\pm}^p$ . However, when the trajectory is shifted by only a quarter of the pitch of the cholesteric helix, the radiation loss (18) on the  $\nu_{+}^p$  boundary of the Čerenkov-forbidden band is found to vanish (see broken curve in Fig. 6b) and becomes infinite when  $\nu = 0, 1$ . Thus, the most rapid variation in the differential radiation loss (18) as a function of the position of the trajectory in space occurs on the boundaries  $\nu = \nu^p = 0, 1, \nu_{\pm}^p$  (from zero to infinity on the boundaries of the 0 and  $\nu_{+}^p$  forbidden bands; see Fig. 6b). This is so because, on these boundaries ( $\nu = \nu^p$ ) waves emitted in the directions  $\mathbf{k}_0$  and  $\mathbf{k}_1$  are found to be identical and differ only by the phase factor  $e^{2i\Phi}$ . In particular,  $|\mathbf{k}_0| = |\mathbf{k}_1|$ , on these boundaries, and the polarization characteristics (5) are also equal:

$$p_{0i} = p_{1i} = \sin \theta \frac{\nu^p + m}{\nu^p - m}, \quad i=1, 2.$$

Thus, the phase of the wave emitted in the direction of  $\mathbf{k}_1(\pi - \varphi)$  (see Fig. 5) also differs from the phase of the wave emitted in the direction of  $\mathbf{k}_0(\varphi)$  by the factor  $e^{2i\Phi}$ . This means that, when the field amplitudes are added for directions of emission with azimuth  $\varphi$  and  $\pi - \varphi$ , the root-type divergence in the differential radiation loss can be suppressed altogether on the boundaries of the forbidden band  $0, \nu_{+}^p$  (see Figs. 6a and b). On the other hand, on the boundaries of the polarization-forbidden bands  $\nu_{-}^p, 1$  the quantities  $\omega_{\pm} = 2f_{\pm} + 2g_{\pm} \cos 2\Phi$  may also vary from zero to infinity (see Fig. 6a), but the total radiation loss  $w = w_{+} + w_{-}$  does not vanish identically (see Fig. 6b) because these boundaries lie in the region in which emission is not forbidden.

Let us now examine in detail the nature of the azimuthal dependence of the differential loss  $d^2W/d\omega d\varphi$  for small deviations of the angle  $\varphi$  near the point on the cone with azimuth  $\varphi = 0$ . Bearing in mind the dependence of the Bragg frequency  $\omega_B$  on the azimuth in (3a), we find that the frequency detuning is given by

$$\nu = 2(1+m) \sin^2 \psi_0 \left( \frac{\omega - \omega_B^{\min}}{\omega_B^{\min}} - \frac{\varphi^2}{2} \right) \delta^{-1}, \quad (19)$$

$$\omega_B^{\min} = c\tau \left[ 2\epsilon^{1/2} \left( 1 - \frac{\delta}{4} \cos^2 \psi_0 \right) \sin \psi_0 \right]^{-1}.$$

Hence, it follows that the differential loss (18) is independent of the azimuth  $\varphi$  in the angular interval  $|\varphi| \sim \delta$ , i.e., in this interval, the dependence of the radiation loss (18) on frequency is the same. This result shows that the observed features (the forbidden band into which emission cannot take place and the root-type divergences on the boundaries of this band) can be additionally enhanced when integrated with respect to the azimuth (in the interval  $|\varphi| \sim \delta$ ). The dependence on azimuth begins to be significant only for  $|\varphi| \sim \delta^{1/2}$ . Accordingly, the dependence of  $d^2W/d\omega d\varphi$  on the azimuth is found to be substantially (by a factor of the order of  $\delta^{1/2}$ ) broadened as compared with the corresponding frequency dependence when expressed as a function of  $\Delta\omega/\omega$ .

As the frequency is reduced, the regions in which the wave vectors  $\mathbf{k}_0(\varphi)$  and  $\mathbf{k}_0(-\varphi)$  as functions of the azimuth undergo diffraction changes begin to overlap at the point  $\varphi = 0$  on the cone, so that, for frequencies  $\omega \lesssim \omega_B^{\min}$  (see Figs. 5 and 7), the azimuthal dependence of  $d^2W(\varphi)/d\omega d\varphi$  will be essentially different from the corresponding frequency dependence of  $d^2W(\omega)/d\omega d\varphi$ , because the Bragg angle  $\theta_B$  for such frequencies (which determines the direction of strong diffraction scattering) exceeds the angle  $\psi_0$  at which the Čerenkov radiation is emitted (see Fig. 5). Hence, by integrating (18) with respect to the azimuth, one can readily show that the spectral density of the Čerenkov radiation emitted into the frequency region  $\omega \lesssim \omega_B^{\min}$  may differ from the corresponding characteristic of Čerenkov radiation in a homogeneous medium with refractive index  $\epsilon^{1/2}$  by the amount  $\sim \delta^{1/2}$ . However, this difference does not exceed values of the order of  $\sim \delta$  when integration with respect to frequency is performed.

The following conclusion may be drawn from the above discussion: when the spectral resolution of the system used to detect the Čerenkov radiation is better than  $\delta$ , diffraction features will also appear in the radiation loss integrated with respect to the angles  $\psi$  and  $\varphi$ . In fact, analysis of Fig. 7 will show that the ratio of the energy  $\Delta W$  radiated at frequency  $\omega$  to the interval  $\Delta\varphi$  in which this energy is recorded may differ from the value predicted by Eq. (9) by a considerable factor. When the dielectric anisotropy is not too small ( $\delta \sim 0.1-0.01$ ), the interval  $\Delta\varphi \sim \delta^{1/2}$  may reach  $10-12^\circ$  around the point on the cone with azimuth  $\varphi = 0$ . Further increase in the interval  $\Delta\varphi$  in which the radiation of frequency  $\omega$  is recorded will ensure that the difference as compared with (9) will not exceed  $\sim \delta^{1/2}$ .

*Boundary-value problem in the Laue geometry.* When the particle moves at right-angles to the helicoidal axis of the cholesteric crystal, the boundary-value problem for the infinite planar specimen of a cholesteric liquid crystal with faces perpendicular to the helicoidal axis cannot be solved in the usual way in Bragg geometry because the particle does not then cross the boundaries of the specimen. Let us now suppose that the optical (heloidal) axis of the cholesteric is parallel to the faces of the specimen (symmetric Laue geometry) and, without writing out the general expressions for the field amplitudes analogous to (12), let us consider some general results. The radiation intensities emitted into the Čerenkov and diffraction cones and integrated over the polar angle

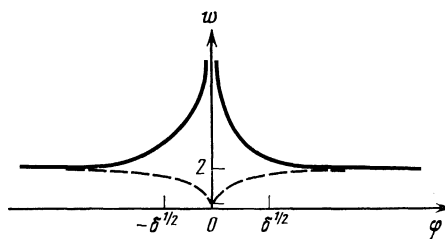


FIG. 7. Azimuthal dependence  $w(\varphi)$  at frequency  $\omega = \omega_B [1 + \delta\nu - \nu^p / 2(1 - m)]$ . The function  $w(\varphi)$  at this frequency corresponds to the frequency function  $w(\nu)$  of Fig. 6b, c, and d in the region  $\nu < \nu^p$ . Solid curve— $\Phi = 0$ , dashed curve— $\Phi = \pi/2$ .

$\psi$  are, of course, equal in this case ( $I_c = I_d$ ) and in the Čerenkov-forbidden band  $I_c = I_d \simeq 0$ . The frequency (angular) dependence of the intensities  $I_c, I_d$  is essentially the same as the corresponding frequency and angle dependence of the differential radiation loss  $d^2W/d\omega d\varphi$  (Fig. 6b, c, and d). When the CLC specimen has a finite thickness, the square-root singularity in the differential radiation loss (18) is replaced by an intensity maximum which exceeds by a factor of about  $(\delta L/p)^{1/2}$  the intensity emitted in the homogeneous medium.

## CONCLUSION

The above analysis of the Vavilov-Čerenkov radiation in first-order diffractive reflection in cholesteric liquid crystals shows that this radiation undergoes a relatively complicated spatial and frequency redistribution. The intensity of the wave emitted in the Bragg geometry by a planar CLC specimen near the diffractive-reflection boundary is of the order of the fourth power of the specimen thickness. The position of the maxima [see (14)–(16)] is unaffected when transition radiation and even dielectric reflection by the specimen boundaries are taken into account because these maxima are of diffraction origin.

Experimental studies of the Čerenkov-forbidden bands are possible if the frequency  $\Delta\omega/\omega$  and azimuthal ( $d\varphi$ ) resolution is of the order of or less than the dielectric anisotropy  $\delta$ . When the plane of diffraction scattering coincides with the plane defined by the optical axis and the velocity vector, the azimuthal resolution satisfies the less stringent condition  $d\varphi \sim \delta^{1/2}$ . When this is so, the ratio of the radiated energy at frequency  $\omega$  to the interval  $\Delta\varphi$  in which this energy is recorded may differ by a substantial factor from the corresponding

quantity in a homogeneous medium, given by (9). When the dielectric anisotropy is not too small ( $\delta \sim 0.01$ – $0.1$ ), the interval  $\Delta\varphi$  may reach values of  $10$ – $12^\circ$  near the point with azimuth  $\varphi = 0$  on the Čerenkov cone.

The author is greatly indebted to V. A. Belyakov for useful discussions of the results and for his interest in this research, and to V. E. Dmitrienko for useful suggestions.

- <sup>1</sup>E. I. Kats, Zh. Eksp. Teor. Fiz. **61**, 1686 (1971) [Sov. Phys. JETP **34**, 912 (1971)].
- <sup>2</sup>V. A. Belyakov, V. E. Dmitrienko, and V. P. Orlov, Pis'ma Zh. Tekh. Fiz. **1**, 978 (1975) [Sov. J. Tech. Phys. Lett **1**, 422 (1975)].
- <sup>3</sup>N. V. Shipov and V. A. Belyakov, Zh. Eksp. Teor. Fiz. **75**, 1589 (1978) [Sov. Phys. JETP **48**, 802 (1978)].
- <sup>4</sup>F. G. Bass and V. M. Uakovenko, Usp. Fiz. Nauk **86**, 189 (1965) [Sov. Phys. Usp. **8**, 420 (1965)].
- <sup>5</sup>K. F. Casey, C. Jen, and Z. A. Kaprielian, Phys. Rev. **140**, B768 (1965).
- <sup>6</sup>A. I. Smirnov and V. V. Fedorov, Zh. Eksp. Teor. Fiz. **76**, 866 (1979) [Sov. Phys. JETP **49**, 436 (1979)].
- <sup>7</sup>I. M. Dykman and L. A. Prokhnitskii, Fiz. Tverd. Tela (Leningrad) **22**, 2420 (1980) [Sov. Phys. Solid State **22**, 1408 (1980)].
- <sup>8</sup>L. D. Landau and E. M. Lifshitz, Elektrodinamika sploshnykh sred (Electrodynamics of Continuous Media), Nauka, Moscow, 1982, Sec. 115.
- <sup>9</sup>V. A. Belyakov and A. S. Sonin, Optika kholestericheskikh zhidkikh kristallov (Optics of Cholesteric Liquid Crystals), Nauka, Moscow, 1982.
- <sup>10</sup>V. A. Belyakov and N. V. Shipov, Zh. Eksp. Teor. Fiz. **82**, 1159 (1982) [Sov. Phys. JETP **55**, 674 (1982)].
- <sup>11</sup>A. M. Afanas'ev and M. A. Aginyan, Zh. Eksp. Teor. Fiz. **74**, 570 (1978) [Sov. Phys. JETP **47**, 300 (1978)].
- <sup>12</sup>V. A. Bazylev and N. K. Zhevago, Usp. Fiz. Nauk **137**, 605 (1982) [Sov. Phys. Usp. **25**, 565 (1982)].
- <sup>13</sup>S. V. Shiyonovskii, Ukr. Fiz. Zh. **27**, 361 (1982).

Translated by S. Chomet